institut de physique nucléaire

CNRS - IN2P3 - UNIVERSITÉ PARIS - SUD

I.P.N. BP n°1 - 91406 ORSAY

KR8902H92

We regret that some of the pages in the microfiche copy of this report may not be up to the proper legibility standards, even though the best possible copy was used for preparing the master fiche.

IPNO - DRE 89-07

SPIN-FLIP TRANSITIONS IN ^{46}Ti, ^{48}Ti AND ^{50}Cr EXCITED BY INELASTIC PROTON SCATTERING*

A. WILLIS, M. MORLET, N. MARTY, C. DJALALI
Institut de Physique Nucléaire, Orsay, BP N°1, 91406 France
D. BOHLE†, A. RICHTER and H. STEIN
Institut für Kernphysik der Technischen Hochschule Darmstadt
6100 Darmstadt, Fed. Rep. Germany

Spin-flip transitions in ^{46}Ti, ^{48}Ti and ^{50}Cr excited by inelastic proton scattering*

A. Willis, M. Morlet, N. Marty, C. Djalali
Institut de Physique Nucléaire
Orsay BP N° 1, 91406 France

D. Bohle† A. Richter and H. Stein
Institut für Kernphysik
der Technischen Hochschule Darmstadt
6100 Darmstadt, Fed. Rep. Germany

Abstract

Forward angle cross sections for 1^+ states have been measured in the non closed shell nuclei ^{46}Ti, ^{48}Ti, ^{50}Cr by 201 MeV proton inelastic scattering. The total measured 1^+ strength is compared with microscopic distorted wave impulse approximation calculations using large scale shell model wave functions. The quenching for the 1^+ strength ranges from 0.3 to 0.5 . For the low energy isovector 1^+ states the ratio of the orbital to the spin excitation is extracted.

NUCLEAR REACTIONS ^{46}Ti, ^{48}Ti, ^{50}Cr (p,p'), E=201 MeV; measured $d\sigma/d\Omega$, θ=3°-8°. Deduced $J^\pi=1^+$ levels and transition strengths.

*Supported in part by the Deutsche Forschungsgemeinschaft

†Present address: DFVLR, D-5000 Köln, Fed. Rep. Germany

1 Introduction

During the last few years, spin excitations in nuclei have been extensively studied both theoretically and experimentally, using different probes. The presence of isovector $\Delta L=0$ spin-flip transitions has been firmly established in all the studied nuclei. A common property of such excitations is that there is generally a discrepancy (up to a factor of 3 in some cases) between the predicted and the observed strength which is refered to as quenching.

In (e,e'), (γ,γ') and some recent (p,p') experiments, almost no quenching was found for ligth nuclei in the s-d shell [1] while in a (p,n) experiment a quenching of 0.6 was found for the same nuclei [2]. In nuclei heavier than ^{40}Ca, the (p,p') data indicate a quenching of 0.3 to 0.4 [3] while the (p,n) data give a quenching of 0.5 to 0.6 [4].

Beside these spin-flip transitions which are described in terms of particle-hole excitations, recently a new kind of low energy $J^{\pi}=1^{+}$ states excited through a mainly dipole mode, sometimes called "scissors mode", has been predicted in deformed even-even nuclei [5]. This moderately collective mode had been first discovered in (e,e') scattering in heavy deformed nuclei [6] and late confirmed by (γ,γ')measurements [7]. After the suggestion that similar excitations with large orbital components should also exist in light non-closed shell nuclei [8] they have subsequently been observed [9] in (e,e') and (p,p') experiments on ^{46}Ti. A comprehensive summary on the present status of the scissors mode is given in ref.[10].

The present experiment is the study of $\Delta L=0$, $\Delta S=1$ transitions in the three non-closed f-p shell nuclei ^{46}Ti, ^{48}Ti, ^{50}Cr by (p,p') inelastic scattering at 201 MeV. The motivation of the experiment was twofold.

Firstly, similarly as in ^{46}Ti [9] to study the low lying 1^{+} states in ^{48}Ti and ^{50}Cr and to extract the ratio of the orbital to the spin contributions in the electromagnetic excitation of these states. These ratios are obtained by combining the (e,e') results with the present (p,p') data. They are compared to predictions from different models. In the present paper we will only briefly discuss the results on those low lying 1^{+} states; a complete discussion will be given in a forthcoming paper [11].

Secondly, to measure the total $\Delta L=0$ spin-flip strength in the three nuclei and to study the variation of the quenching in the f-p shell by com-

parison to shell model calculations [12].

2 Experimental procedure

The measurements were carried out using the 201 MeV proton beam at the Orsay synchrocyclotron. The set-up which allows to get data at small angles (2° and 3°) with very low background has been described previously [13].

The target thicknesses were 11.83 mg/cm^2 for ^{46}Ti, 11.81 mg/cm^2 for ^{48}Ti and 33.5 mg/cm^2 for ^{50}Cr. The isotopic enrichement was 81.2% for ^{46}Ti with 14.5% of ^{48}Ti; 99.1% for ^{48}Ti and 90.12% for ^{50}Cr with 8.82% of ^{52}Cr.

The angular range covered was from 3° to 8° by 1° steps and the excitation energy range scanned was from 3 to 15 MeV. The overall energy resolution was 70 keV for the Ti targets and about 110 keV for ^{50}Cr. The absolute cross sections were obtained by reference to the free (p,p) cross section measured on a $(CH_2)_n$ target in the same experimental conditions; an error less than 5 % is assumed for the normalisation which is not included in the error bars of the cross section data.

3 Theoretical models

Two models which will be called I and II are available for the ΔL=0, ΔS=1 transitions in ^{46}Ti, ^{48}Ti and ^{50}Cr. In model I [14] there are fourteen independent single-particle matrix elements corresponding to the jj' combinations $0f_{7/2} - 0f_{7/2}$, $0f_{7/2} - 0f_{5/2}$, $0f_{5/2} - 0f_{5/2}$, $1p_{3/2} - 1p_{3/2}$, $1p_{3/2} - 1p_{1/2}$, $1p_{1/2} - 1p_{1/2}$, $0f_{5/2} - 1p_{3/2}$ for the ΔT=0 (isoscalar) and the ΔT=1 (isovector) couplings.

For model II [15] the individual wave functions were not avaliable, we only have the B(ℓ), B(σ) and B(M1) values for the $T_0 \rightarrow T_0$ and the $T_0 \rightarrow T_0 + 1$, 1^+ transitions.

Using model I, microscopic DWIA (Distorted Wave Impulse Approximation) calculations have been performed with the code RESEDA [16] taking the nucleon-nucleon interaction from the Arndt phase shifts [17]. The op-

tical potential parameters obtained from the parametrization of Schwandt [18] were used.

When a state is excited through an interaction with a well defined isospin, as for the low energy 1^+ state which is excited through a pure isovector $\Delta S=1$ interaction, it is possible [9,13] to extract the electromagnetic spin transition probability $B(\sigma)$ from the (p,p') cross section extrapolated to a momentum transfer q=0 fm^{-1}. This method cannot be applied to transitions which are not pure in isospin, i.e. transitions which are of mixed isoscalar and isovector character.

The B(M1) value wich is measured in electromagnetic reactions is related to the $B(\sigma)$ value through the relation $B(M1)=(\sqrt{B(\ell)} \pm \sqrt{B(\sigma)})^2$. Combining the $B(\sigma)$ value extracted from the (p,p') experiment with the measured B(M1) value, the ratio $B(\ell)/B(\sigma)$ can be extracted. In principle there are two different possible values for $B(\ell)$ according to the choice of the plus or minus sign in the above formula. But, as both models I and II give the plus sign for the excitation of the low lying state of the three nuclei this sign has been taken to extract the $B(\ell)$ values in the present paper.

4 Experimental results and discussion

4.1 Data reduction

The spectra taken at very forward angles like 3^o or 4^0 show a continuum which appears like a tail of the elastic peak, but which is due to the rescattering of the elastically scattered beam. This background is important at the excitation energy of the "scissors mode like" 1^+ states; it could be partly reduced by setting windows on both the vertical and horizontal angles of the trajectories. The remaining background in this energy region has been subtracted as described in ref. [19].

The analysis of the peaks was done by applying a fitting procedure, the shape of well separated peaks appearing in the same spectrum was taken as a reference. In order to optimize the fit, the shape of the continuum in the high excitation energy part of the spectrum has been chosen so that the shape of the reference peak could fit some isolated peaks in this region. Two different continua are given as an example in fig. 1. The continua

used for the other spectra are given in figs. 4 and 7. The main error on the quenching comes from the estimate of this continuum.

The energy calibration has been performed by reference to well known states which are strongly excited in the spectra.

The excitations due to the impurity of ^{48}Ti in the ^{46}Ti target were subtracted by using the ^{48}Ti data measured in the present experiment; for ^{50}Cr the results were corrected for the ^{52}Cr impurity using previous results [12].

4.2 ^{46}Ti

A spectrum taken at a laboratory angle of 4° is shown in fig. 1. The 1^+ states are labeled by arrows. The energy of the peaks was fixed by reference to the energy of the first excited state at 2.96 MeV. The analysis of the peaks was limited up to 13.35 MeV excitation energy and for many of them a fitting procedure was applied (taking as a reference the shape of the peak at 8.46 MeV). The limit of the cross section for detection of 1^+ states is approximately 50 μb at 3°. Thus, due to the strong fragmentation of the 1^+ strength, some states in the analyzed region might be missed.

In table 1 the excitation energies and cross sections measured at 3° are given.

Angular distributions for the low energy 1^+ state located at 4.32 MeV, for the 8.46 MeV state and for the total cross section summed over all the 1^+ states below 13.35 MeV are shown in fig. 2.

In fig. 3 the experimental (p,p') cross sections measured in this experiment and the (p,p') cross sections predicted by model I are compared . A concentration of strength near 7.5 MeV, due mostly to proton spin-flip states, is observed. The strong 1^+ state located at 8.46 MeV which is also strongly excited in (e, e') scattering [11] is not predicted by model I. Model II has the strongest 1^+ state located at 8.51 MeV with a B(M1) value of 3.148 μ_n^2 and a B(σ) value of 3.540 μ_n^2. We cannot extract the B(σ) value experimentally for such a state which may be excited by the ΔT=0 and ΔT=1 spin interaction.

The experimental centroid energy of the 1^+ states is 9.78 MeV, to be compared to the theoretical value of 9.55 MeV. The total 1^+ cross section

at 3° located below 13.35 MeV is $3.21^{+1.1}_{-0.5}$ mb/sr and the ratio R of the total experimental 1^+ strength to the strength predicted by model I in the same energy range, i.e. the quenching factor, is $R = 0.29^{+0.1}_{-0.05}$.

4.3 ^{48}Ti

A spectrum taken at a laboratory angle of 4° is shown in fig. 4. The low energy 0^+ state at 3.00 MeV, and the 2^+ state at 3.37 MeV [20] were taken as a reference for the energy calibration. The analysis of the data was performed up to 13.5 MeV. For some energy regions with a high density of states, the fitting procedure did not allow to give intensities for separate peaks; in such regions the 1^+ strength was summed over an energy bin.

In table 2 the excitation energies and cross sections measured at 3° for the 1^+ states are given. Data available from (e,e') measurements are also stated for comparison [11]. In the low energy region both models predict a 1^+ isovector state, partly excited by the orbital interaction in electromagnetic reaction, located at 3.75 MeV for model I and 3.63 MeV for model II. The states at 3.74 and 4.26 MeV excited in the present (p,p') experiment and in (e,e') scattering are indeed of this type [11]. The strongly excited state at 5.62 MeV has predominantly a 2^+ angular distribution but some 1^+ contribution cannot be excluded.

The state located at 7.20 MeV is strongly excited by (p,p') as well as by (e,e') scattering. Model I predicts a state at 7.10 MeV with a B(M1)= 1.037 μ_n^2 which is mainly excited through an isovector interaction, the nearby state at 7.40 MeV is a mixture of $\Delta T=0$ and $\Delta T=1$ transitions. Model II predicts $T=T_0$ states at 7.264, 7.477 and 7.813 which are nearly pure spin-flip transitions. As a comparison of state by state is not justified, we cannot extract the $B(\ell)$ contribution for the experimentally excited state at 7.20 MeV.

The experimental and theoretical (p,p') cross sections given by model I at 3° are compared in fig. 5; for the excitation range from 10.5 to 13.5 MeV only cross sections integrated over an energy range could be given. In the experimental data the 1^+ strength is more spread than predicted and there is no gap between the region of 7.5 MeV and the region of 9 to 10 MeV where dominant neutron $(f_{7/2}^{-1} - f_{5/2})$ spin-flip states are expected.

The experimental centroid energy of 1^+ states is 9.34 MeV to be compared to the centroid energy of 10.09 MeV given by model I. Due to the underlying continuum, part of the strength could have been missed above 10 MeV.

The angular distributions for the states at 3.74 MeV, 7.20 MeV and for the 1^+ strength summed over all the states or bumps of energy less than 13.5 MeV are given in fig. 6. The total 1^+ cross section measured at 3°, located below 13.5 MeV is $4.74^{+1.3}_{-0.65}$ mb/sr.

The ratio R of the total experimental 1^+ strength to the total 1^+ strength given by model I in the same energy range, i.e. the quenching factor, is $R=0.36^{+0.1}_{-0.05}$.

4.4 ^{50}Cr

A spectrum taken at a laboratory angle of 4° is shown in fig. 7. The peak taken as a reference for the energies and for the shapes is the 0^+ state at 5.71 MeV. The analysis was limited to a maximum energy of 12.5 MeV. From the angular distribution of the low energy states the following assignments were performed: 1^+ for the state at 3.63 MeV, 0^+ for the state at 4.04 MeV, tentatively 2^+ for the state at 4.19 MeV with perhaps a small 1^+ admixture and tentatively 1^+ for the state at 4.70 MeV.

A low energy 1^+ state is predicted at 3.96 MeV by model I and at 3.85 MeV by model II. Assuming that this state is the experimentally 3.63 MeV state excited by (e,e') as well as by (p,p') scattering the $B(\sigma)$ and the ratio $B(\ell)/B(\sigma)$ were extracted.

The energies and cross sections at 4°, corrected from the ^{52}Cr impurity present in the target, are given in table 3. Except for the "scissors mode" state, there is actually no (e,e') data to compare with. The cross sections at 4° for the 1^+ states detected in the present experiment are given in fig. 8 together with the predictions of model I. There are no main peaks due to proton or neutron spin-flip states and no gap in the excitation region between 7.5 MeV and 12 MeV. The experimental centroid energy is 9.13 MeV compared to 9.51 MeV given by the model, but many small states given by the model lie below the detection threshold. The 1^+ cross section at 4° summed over all the states located below 12.5 MeV is $4.10^{+0.8}_{-0.4}$ mb/sr

and the ratio R of the experimental to the predicted cross section in the same energy range is $0.51^{+0.1}_{-0.05}$. The angular distribution for the summed cross section below 12.5 MeV is given in fig. 9.

5 Summary and conclusions

Some general conclusions can be drawn from the (p,p') data presented in this paper, by comparison with (e,e') data when available and with the theoretical predictions of model I and II.

For the three non-closed $f_{7/2}$ shell nuclei ^{46}Ti, ^{48}Ti, ^{50}Cr there is at least one low energy ΔS=1, ΔT=1 state. The experimental B(σ) values and the ratio of the orbital to spin excitation B(ℓ)/B(σ) are given in table 4. The predictions for the two models are also given. These results will be discussed in more detail elsewhere [11], but it should already be remarked here that there is a real discrepancy between experiment and theory in particular in the particle-hole cross conjugate nuclei ^{46}Ti and ^{50}Cr.

For the spin-flip states, as predicted by model I, the location of mainly proton spin-flip states near 7.5 MeV and neutron spin-flip states between 10 and 11 MeV in ^{46}Ti is smeared out when increasing the number of nucleons in the $f_{7/2}$ shell from ^{46}Ti to ^{50}Cr. The same trend has been observed for the nuclei N=28 when going from ^{50}Ti to ^{54}Fe [12,21].

The summed cross section at $\theta_{cm} = 4^o$ increases from $2.4^{+0.8}_{-0.4}$ mb/sr for ^{46}Ti to $3.3^{+1.1}_{-0.55}$ for ^{48}Ti and $4.1^{+0.8}_{-0.4}$ for ^{50}Cr.

The ratio R=$(d\sigma/d\Omega)_{exp}/(d\sigma/d\Omega)_{theor}$ for the three nuclei is given in table 5. The value for ^{50}Ti measured in a preceding experiment [12] is also included; R appears to increase when adding neutrons to the $f_{7/2}$ shell. The spin-flip strength is extremely fragmented.

These results can be compared with data obtained on the Ca isotopes in (e,e') experiments where the M1 strengths -although strongly fragmented in ^{40,42,44}Ca and only strongly concentrated in ^{48}Ca- increases with neutron number (see fig. 14 of ref.[21]. The same kind of results was obtained in (p,p') scattering [13].

Two effects can possibly explain the trend of the data, the extreme fragmentation of the spin-flip strength for N=24 nuclei and ground-state correlations (n particles, n holes) which account of the 1^+ transitions in

^{40}Ca and for the general over prediction of spin-flip strength for all the medium heavy nuclei.

While complete shell-model calculations as the one performed for the nuclei of the s-d shell [1], which give a good account of the $\Delta L=0$, $\Delta S=1$ strength in these nuclei, are not available for heavier nuclei starting at Ca, only little can still be said about the significance of the sizable quenching factor determined in the present work. A first step of improving the situation would certainly be RPA calculations which introduce at least p-h correlations.

Acknowlegments

The authors would like to thank B.A. Brown and T. Oda for communicating their theoretical models and predictions, and D. Goutte for providing us with the ^{50}Cr target. The authors of this article from Darmstadt are grateful to their colleagues from Orsay for their kind hospitality during the experiments.

References

[1] G.M. Crawley, C. Djalali, N. Marty, M. Morlet, A. Willis, N. Anantaraman, B.A. Brown and A. Galonsky, Phys. Rev. C 39 (1989) 311 and references therein.

[2] B.D. Anderson, T.C. Chittrakarn, A.R. Baldwin, C. Lebo, R. Madey, P.C. Tandy, J.W. Watson, C.C. Foster, B.A. Brown and B.H. Wildenthal , Phys. Rev. C 36 (1987) 2195.

[3] N. Marty, in Weak and electromagnetic interactions in nuclei, edited by H.V. Klapdor (Springer, Heidelberg 1986) p. 268.

[4] C.D. Goodman, Spin excitations in nuclei (Plenum, New York, 1984).

[5] N. Lo Iudice and F. Palumbo, Phys. Rev. Lett. 41 (1978) 41.
F. Iachello, Nucl. Phys. A358 (1981) 89c.
E. Lipparini and S. Stringari, Phys. Lett. 130B (1983)139.
F. Iachello Phys. Rev. Lett. 53 (1984) 1427.

[6] D. Bohle, A. Richter, W. Steffen, A.E.L. Dieperink, N. Loludice, F. Palumbo and O. Scholten, Phys. Lett. 137B (1984) 27.
D. Bohle, G. Küchler, A. Richter and W. Steffen, Phys. Lett. 148B (1984) 260.

[7] U.E.P. Berg, C. Bläsing, J. Drexler, R. Heil, U. Kneissl, W. Naatz, R. Ratzek, S. Schennach, R. Stock, T. Weber, H. Wickert, B. Fischer, H. Hollick, and D. Kollewe, Phys. Lett 149B (1984) 59.

[8] L. Zamick Phys. Rev. C 31 (1985)1955 and Phys. Rev. C 33 (1986) 691.

[9] C. Djalali, N. Marty, M. Morlet, A. Willis, J.C. Jourdain, D. Bohle, U. Hartman, G. Küchler, A. Richter, G. Caskey, G.M. Crawley and A. Galonsky, Phys. Lett. 164B (1985) 269.

[10] A. Richter, in: Contemporary topics in nuclear structure physics, edited by R.F. Casten et al. (World Scientific, Singapore 1988) p. 127.

[11] H. Stein et al, to be published.

[12] C. Djalali, N. Marty, M. Morlet, A. Willis, J.C. Jourdain, N. Anantaraman, G.M. Crawley, A. Galonsky and J. Duffy, Nucl. Phys. A410 (1983) 399 and Nucl. Phys. A417 (1984) 564.

[13] C. Djalali, Thesis Orsay (1984), unpublished.

[14] B. A. Brown, private communication.

[15] T. Oda, M. Hino and K. Muto, Phys. Lett. 190 (1987) 14 and T. Oda private communication.

[16] A. Willis, Thesis Orsay (1968), unpublished.

[17] R.A. Arndt, L.D. Roper, R.A. Bryan, R.B. Clark, B.J. VerWest and P. Signell, Phys. Rev. D 28 (1983) 97.

[18] P. Schwandt, H.O. Meyer, W.W. Jacobs, A.D. Bacher, S.E. Vigdor, M.D. Kaitchuck and T.R. Donoghue, Phys. Rev. C 26 (1982) 55.

[19] C. Djalali, N. Marty, M. Morlet, A. Willis, J.C. Jourdain, N. Anantaraman, G.M. Crawley and A. Galonsky, Phys. Rev. C 31 (1085) 758.

[20] Nuclear Data Sheets 45 (1985) 628.

[21] D.I. Sobel, B.C. Metsch, W. Knüpfer, F. Eulenberg, G. Küchler, A. Richter, E. Spamer and W. Steffen, Phys. Rev. C31 (1985) 2054.

FIGURE CAPTIONS

FIG. 1 - Inelastic (p,p') spectrum measured at 4° on ^{46}Ti, 1^+ states are indicated by arrows. Summed peaks are indicated by a bar underneath the arrow. The solid and dashed lines indicate two different shapes of the background subtracted for the determination of the forward angle cross sections for the various 1^+ states.

FIG. 2 - Measured (p,p') angular distributions for the 1^+ states at 4.32 MeV, 8.46 MeV and the total 1^+ strength located below 13.35 MeV in ^{46}Ti. The shape of the angular distributions is compared to microscopic DWIA calculations using model I [14].

FIG. 3 - Predicted cross sections at 3° for the 1^+ states in ^{46}Ti and experimental (p,p') cross sections at the same angle.

FIG. 4 - Inelastic (p,p') spectrum measured at 4° in ^{48}Ti, 1^+ states are indicated by arrows. Summed peaks are indicated by a bar underneath the arrow.

FIG. 5 - Predicted cross sections at 3° for the 1^+ states in ^{48}Ti and experimental (p,p') cross sections at the same angle.

FIG. 6 - Measured (p,p') angular distributions for the 1^+ states at 3.74 MeV, 7.20 MeV and the total 1^+ strength located below 13.5 MeV in ^{48}Ti. The shape of the angular distributions is compared to microscopic calculations using model I [14].

FIG. 7 - Inelastic (p,p') spectrum measured at 4° on ^{50}Cr, 1^+ states are indicated by arrows. Summed peaks are indicated by a bar underneath the arrow.

FIG. 8 - Predicted cross sections at 4° for the 1^+ states in ^{50}Cr and experimental (p,p') cross sections at the same angle.

FIG. 9 - Measured angular distribution for the total 1^+ strength located below 12.5 MeV in ^{50}Cr.

TABLE CAPTIONS

TABLE 1 - Excitation energies and cross sections at 3° for 1^+ states in ^{46}Ti. Data available from the (e,e') experiment are given for comparison.

TABLE 2 - Excitation energies and cross sections at 3° for 1^+ states in ^{48}Ti. Data available from the (e,e') experiment are given for comparison.

TABLE 3 - Excitation energies and cross sections at 4° for 1^+ states in ^{50}Cr. Data available from the (e,e') experiment are given for comparison.

TABLE 4 - $B(\sigma)$ and orbital to spin ratios for the low energy 1^+ transitions in ^{46}Ti, ^{48}Ti and ^{50}Cr.

TABLE 5 - Ratios of experimental to theoretical 1^+ strengths in the even isotopes of Ti and in ^{50}Cr. The value for ^{50}Ti is taken from ref [12].

(p,p')[a]		(e,e')[b]	
E_x	$(d\sigma/d\Omega)_{3^\circ}$	E_x	B(M1)
(MeV)	(μb/sr)	(MeV)	(μ_n^2)
4.32	88±10	4.324	1.04±0.10
6.36	156±17	6.398	0.90±0.10
7.18	60±10		
7.41	98±15		
7.63	160±15		
7.73	155±25		
8.46	219±15		
(8.90-9.10)	215±30		
9.17	75±10		
9.42	160±15		
9.55	80±10		
9.67	134±10		
9.77	43±15		
9.87	74±25		
10.00	79±25		
10.18	112±24		
10.35	87±25		
11.05	141±40		
11.45	160±40		
11.57	104±25		
11.84	106±25		
(12.00-12.40)	400±100		
12.65	37±15		
13.07	108±25		
13.31	104±20		

Table 1 ^{46}Ti a) Present experiment b) Ref. [11].

(p,p')[a]		(e,e')[b]	
E_x	$(d\sigma/d\Omega)_{3^\circ}$	E_x	B(M1)
(MeV)	(μb/sr)	(MeV)	(μ_n^2)
3.74	125±45	3.741	0.50±0.08
4.26	95±30	4.263	0.24±0.10
		5.64	0.50±0.08
6.38	70±7		
6.79	70±7		
6.97	143±14		
7.20	270±20	7.22	0.80±0.06
7.40	90±10		
7.58	114±11		
7.75	110±11		
8.15	189±20		
8.30	316±43	8.37	0.10±0.04
		8.45	0.10±0.03
(8.86-9.00)	490±50		
9.26	220±20		
9.91	127±20		
(10.07-10.23)	238±40		
10.46	224±30		
(10.69-11.07)	324±50		
(11.10-11.30)	183±40		
(11.30-11.60)	160±50		
(11.60-12.00)	204±50		
(12.00-12.55)	244±60		
(13.00-13.55)	213±60		

Table 2 : ^{48}Ti a) Present experiment b) Ref. [11].

(p,p')[a]		(e,e')[b]	
E_x	$(d\sigma/d\Omega)_{4^\circ}$	E_x	B(M1)
(MeV)	(μb/sr)	(MeV)	(μ_n^2)
3.63	170±14	3.630	1.10±0.06
4.70	116±20		
7.34	143±20		
7.61	110±16		
7.78	85±20		
7.98	254±25		
8.27	217±30		
8.50	238±35		
8.65	203±30		
9.01	216±30		
9.19	182±40		
9.40	260±30		
9.57	131±21		
9.71	334±40		
9.90	170±30		
10.11	128±35		
10.24	111±30		
10.38	89±30		
10.52	130±30		
10.82	170±20		
11.02	50±15		
11.18	120±30		
11.66	70±30		
11.82	144±25		
(12.10-12.45)	194±60		

Table 3 : ^{50}Cr a) Present experiment b) Ref. [11].

Nucleus	Experimental results			Theoretical predictions			
				Model I		Model II	
	E_x	$B(\sigma)$	$B(\ell)/B(\sigma)$	E_x	$B(\ell)/B(\sigma)$	E_x	$B(\ell)/B(\sigma)$
^{46}Ti	4.32	0.12±0.03	3.78±1.20	3.93	0.62	4.109	0.74
^{48}Ti	3.74	0.16±0.03	0.51±0.27	3.75	0.71	3.63	0.93
	4.26	0.08±0.03	0.54±0.50				
^{50}Cr	3.63	0.44±0.05	0.34±0.10	3.96	0.89	3.85	0.96

Table 4

Nucleus	^{46}Ti	^{48}Ti	^{50}Ti	^{50}Cr
R	$0.29^{+0.1}_{-0.05}$	$0.36^{+0.1}_{-0.05}$	$0.39^{+0.08}_{-0.04}$	$0.51^{+0.1}_{-0.05}$

Table 5

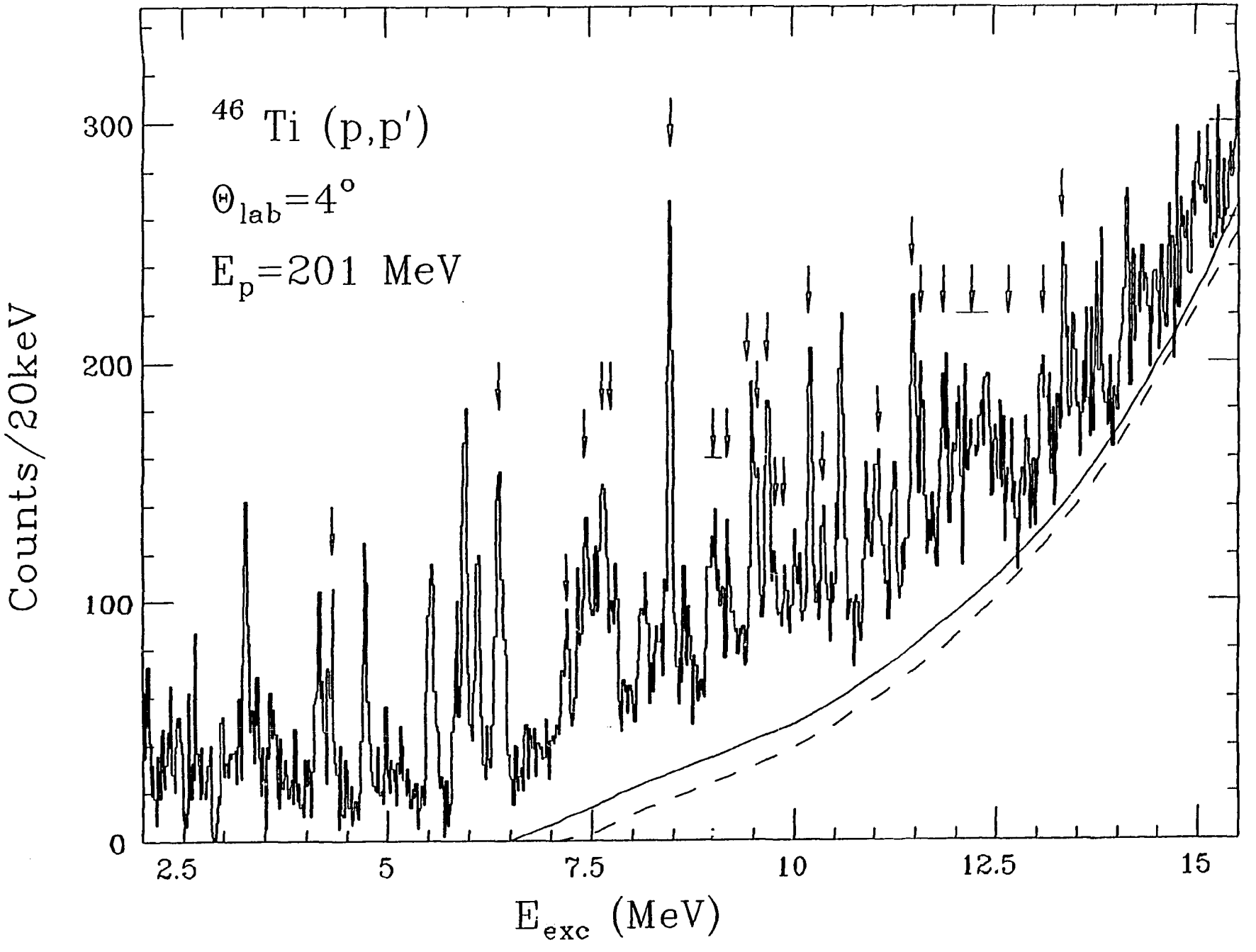
^{46} Ti (p,p′)
Θ_{lab}=4°
E_p=201 MeV
Counts/20keV
300
200
100
0
2.5
5
7.5
10
12.5
15
E_{exc} (MeV)

Fig 2

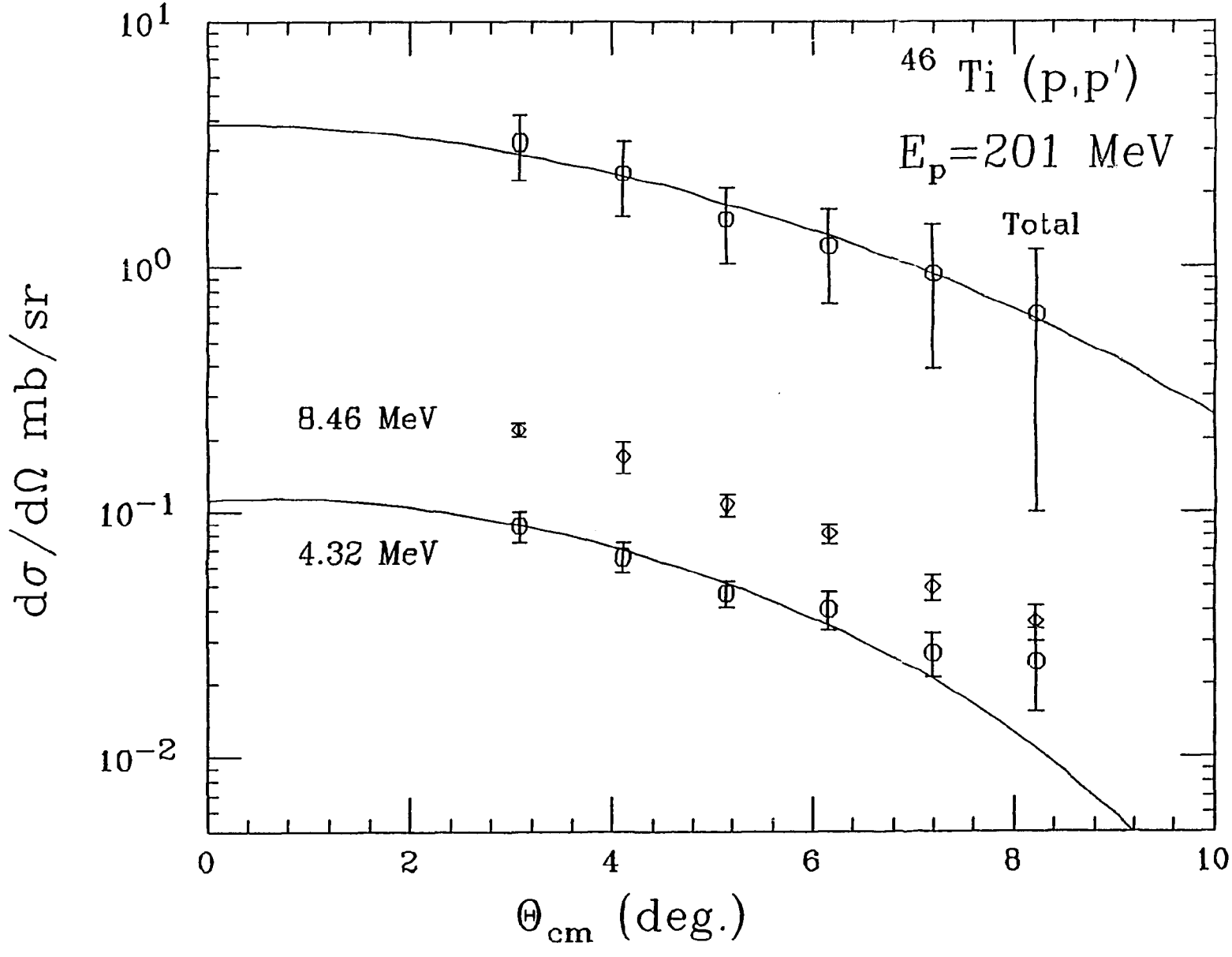
46 Ti (p,p')
E_p=201 MeV
Total
8.46 MeV
4.32 MeV
dσ/dΩ mb/sr
Θ_cm (deg.)
10^1
10^0
10^-1
10^-2
0
2
4
6
8
10

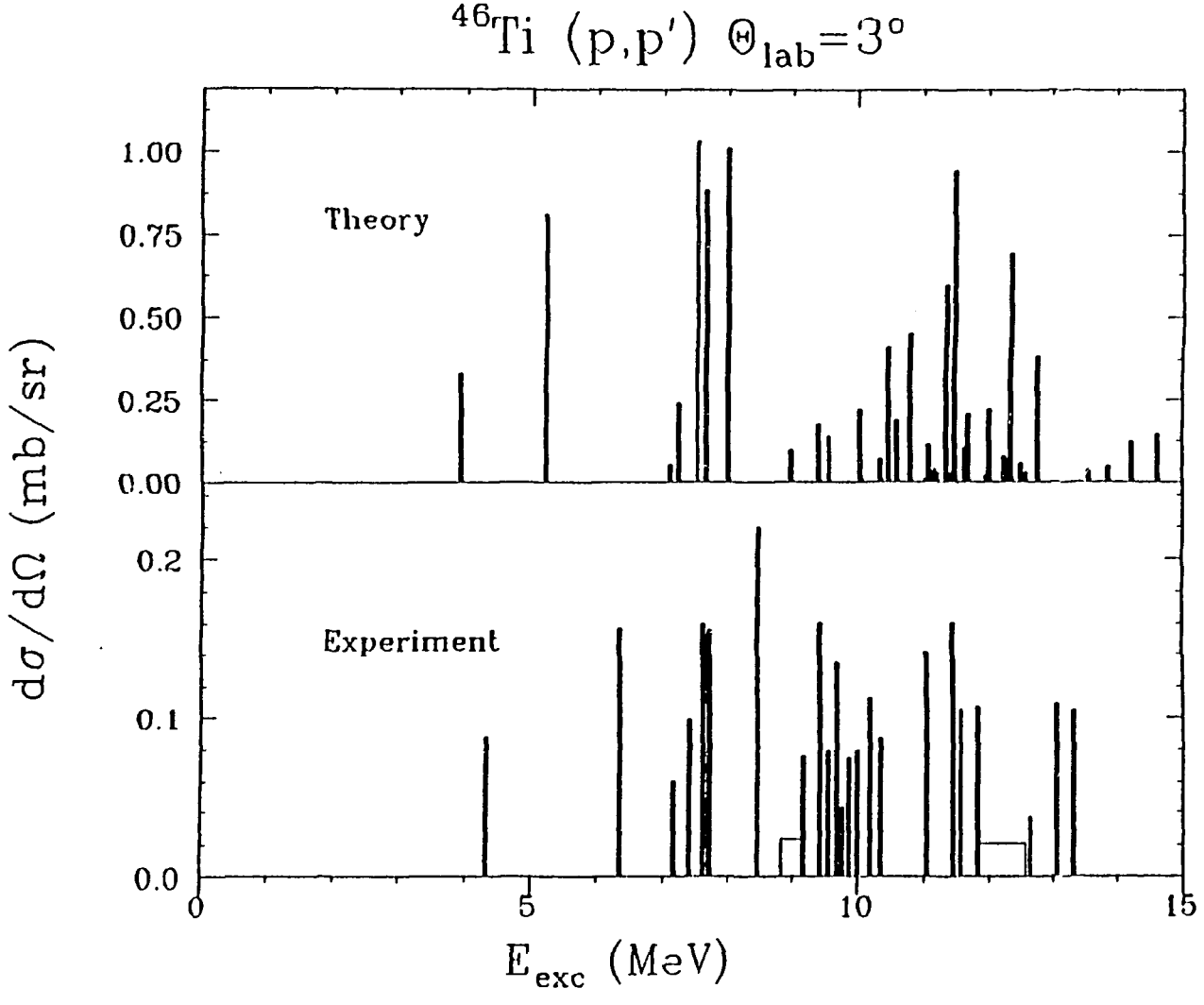
^{46}Ti (p,p') Θ_{lab}=3°
Theory
Experiment
dσ/dΩ (mb/sr)
1.00
0.75
0.50
0.25
0.00
0.2
0.1
0.0
0
5
10
15
E_{exc} (MeV)

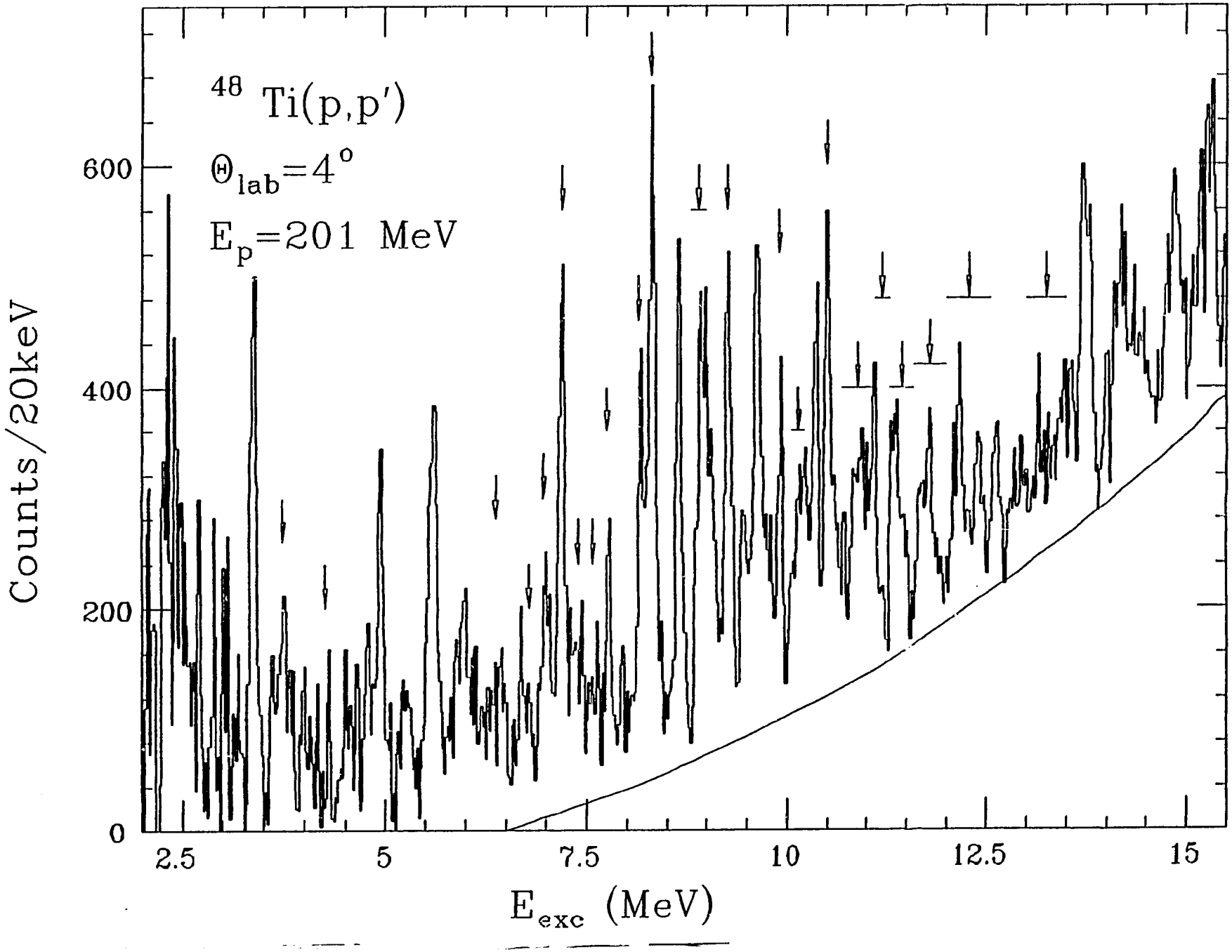
^{48} Ti(p,p′)
$\Theta_{lab}=4^{o}$
E_p=201 MeV
Counts/20keV
0
200
400
600
2.5
5
7.5
10
12.5
15
E_{exc} (MeV)

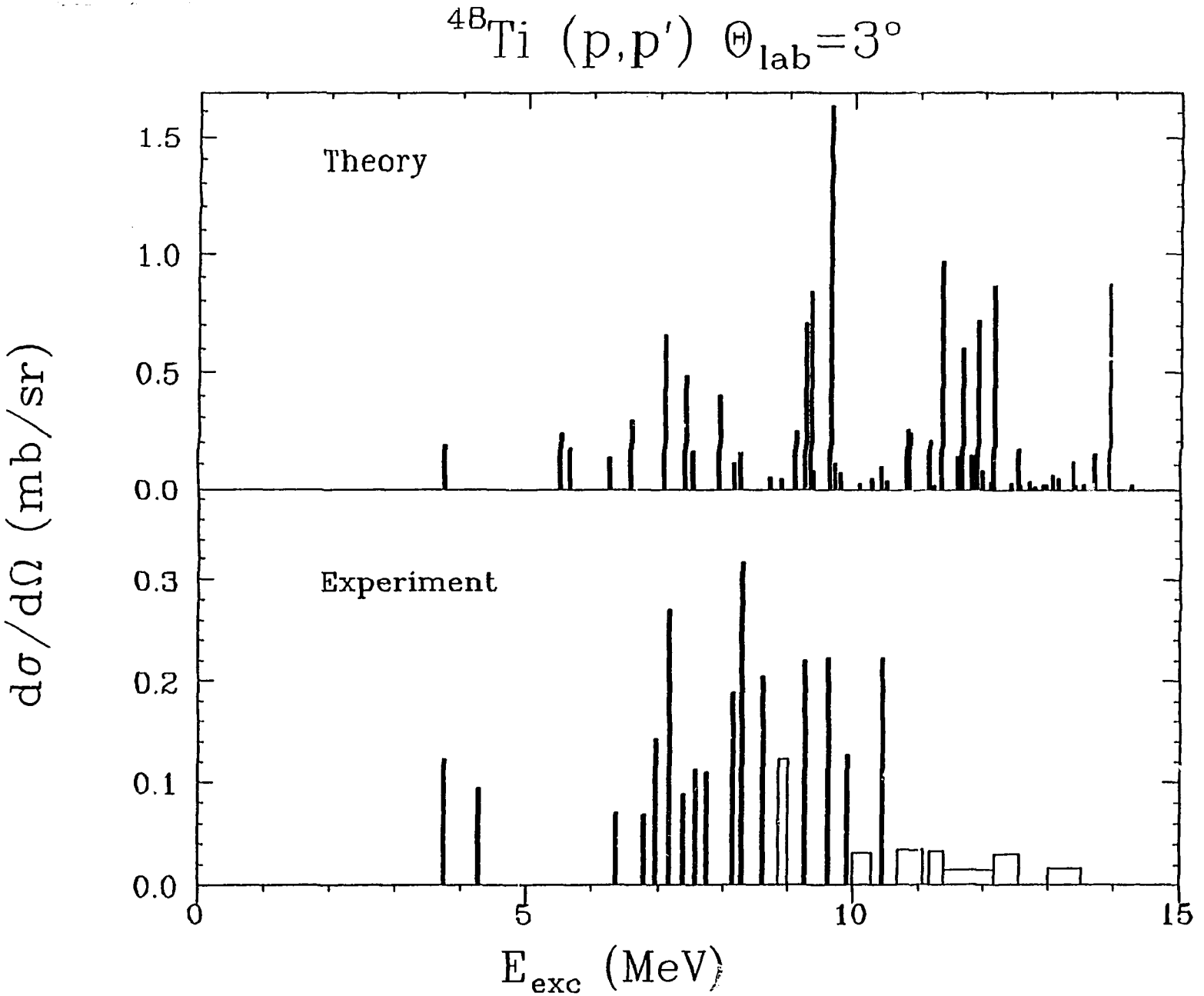
^{48}Ti (p,p′) Θ_{lab}=3°
Theory
Experiment
dσ/dΩ (mb/sr)
E$_{exc}$ (MeV)
1.5
1.0
0.5
0.0
0.3
0.2
0.1
0.0
0
5
10
15

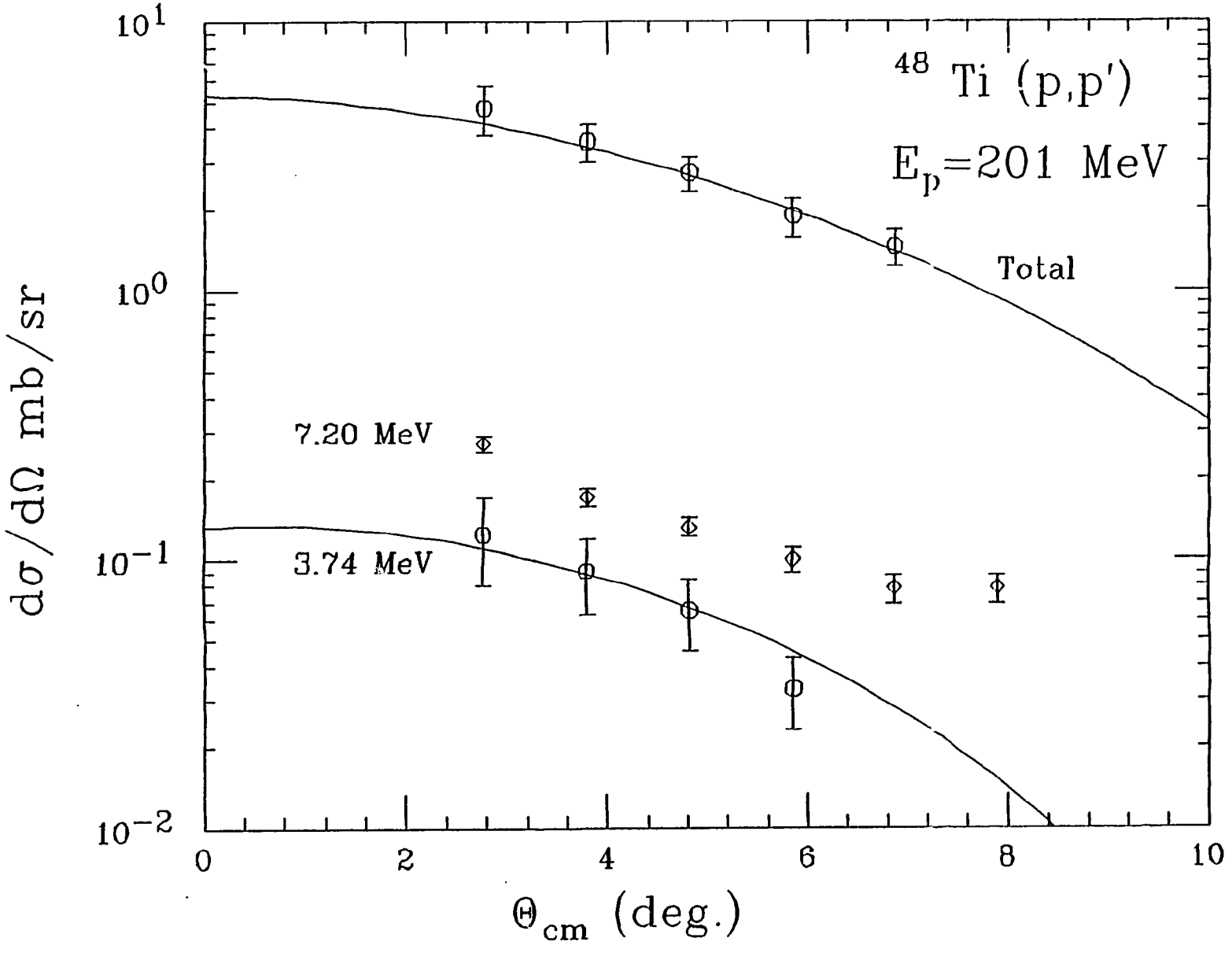
10^1
10^0
10^{-1}
10^{-2}
$d\sigma/d\Omega$ mb/sr
^{48} Ti (p,p')
E_p=201 MeV
Total
7.20 MeV
3.74 MeV
0
2
4
6
8
10
Θ_{cm} (deg.)

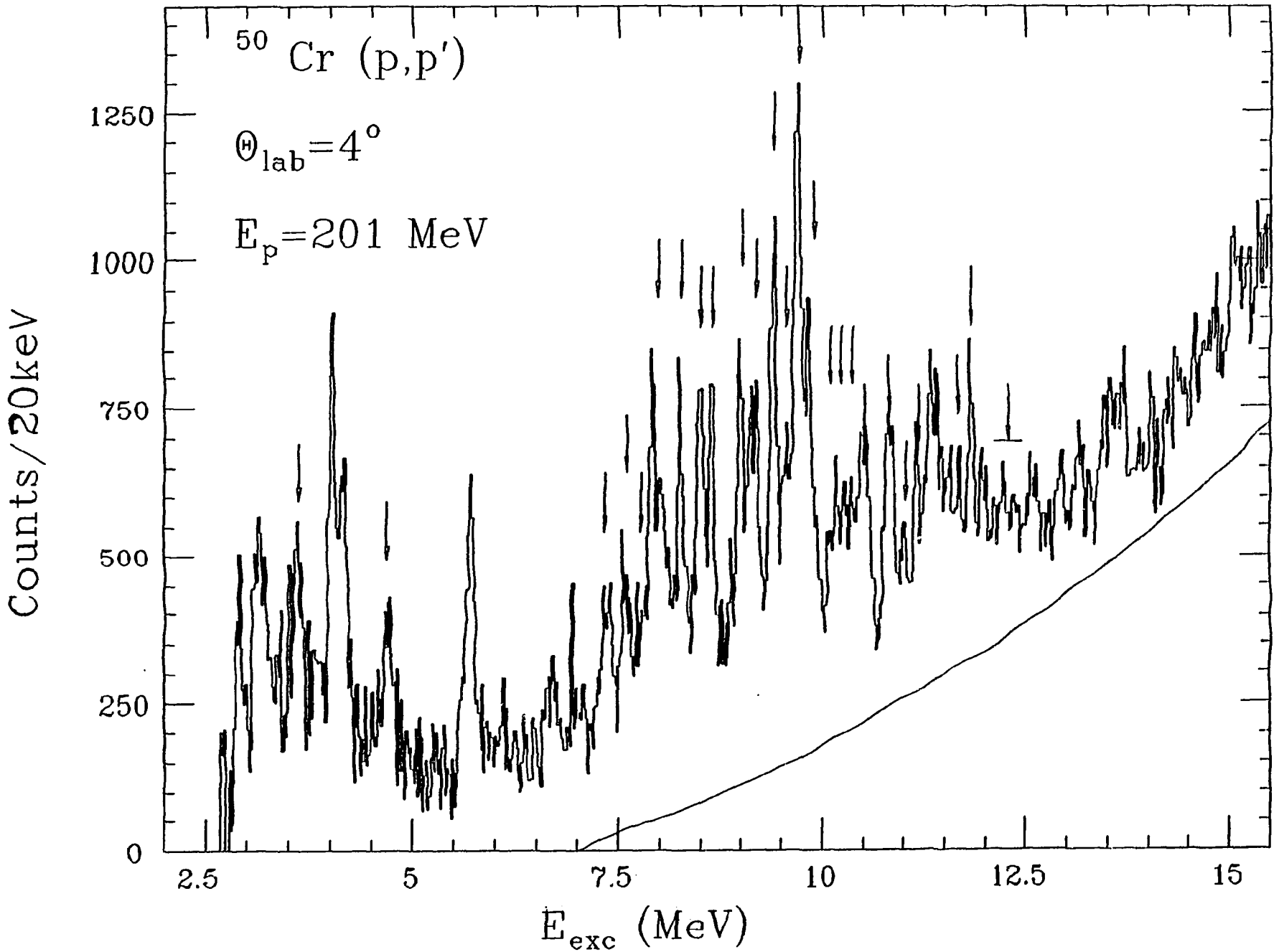
^{50} Cr (p,p')
$\Theta_{lab}=4^{\circ}$
$E_p=201$ MeV
Counts/20keV
0
250
500
750
1000
1250
2.5
5
7.5
10
12.5
15
E_{exc} (MeV)

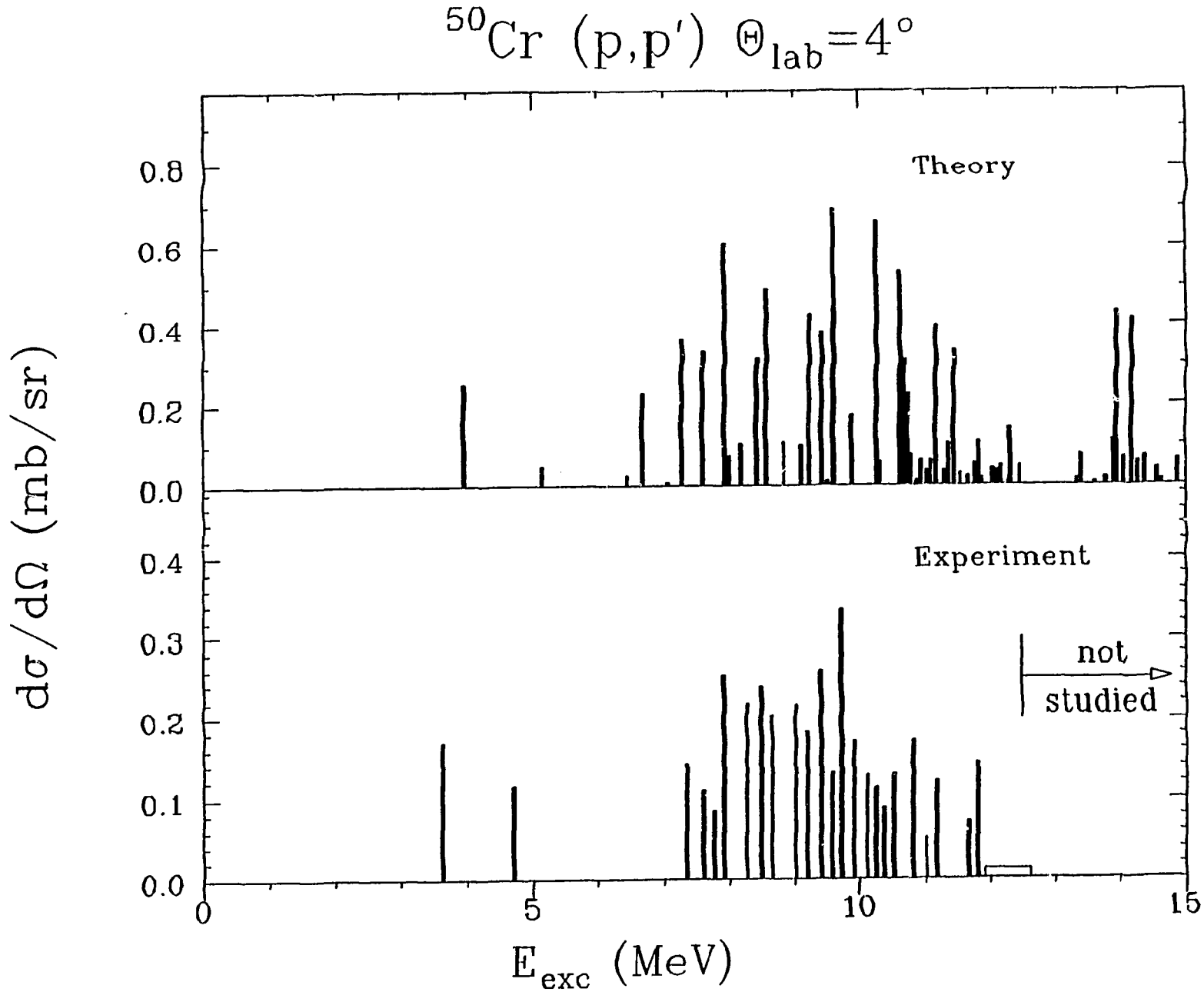
^{50}Cr (p,p') Θ_{lab}=4°
Theory
Experiment
not
studied
0.8
0.6
0.4
0.2
0.0
0.4
0.3
0.2
0.1
0.0
0
5
10
15
dσ/dΩ (mb/sr)
E_{exc} (MeV)

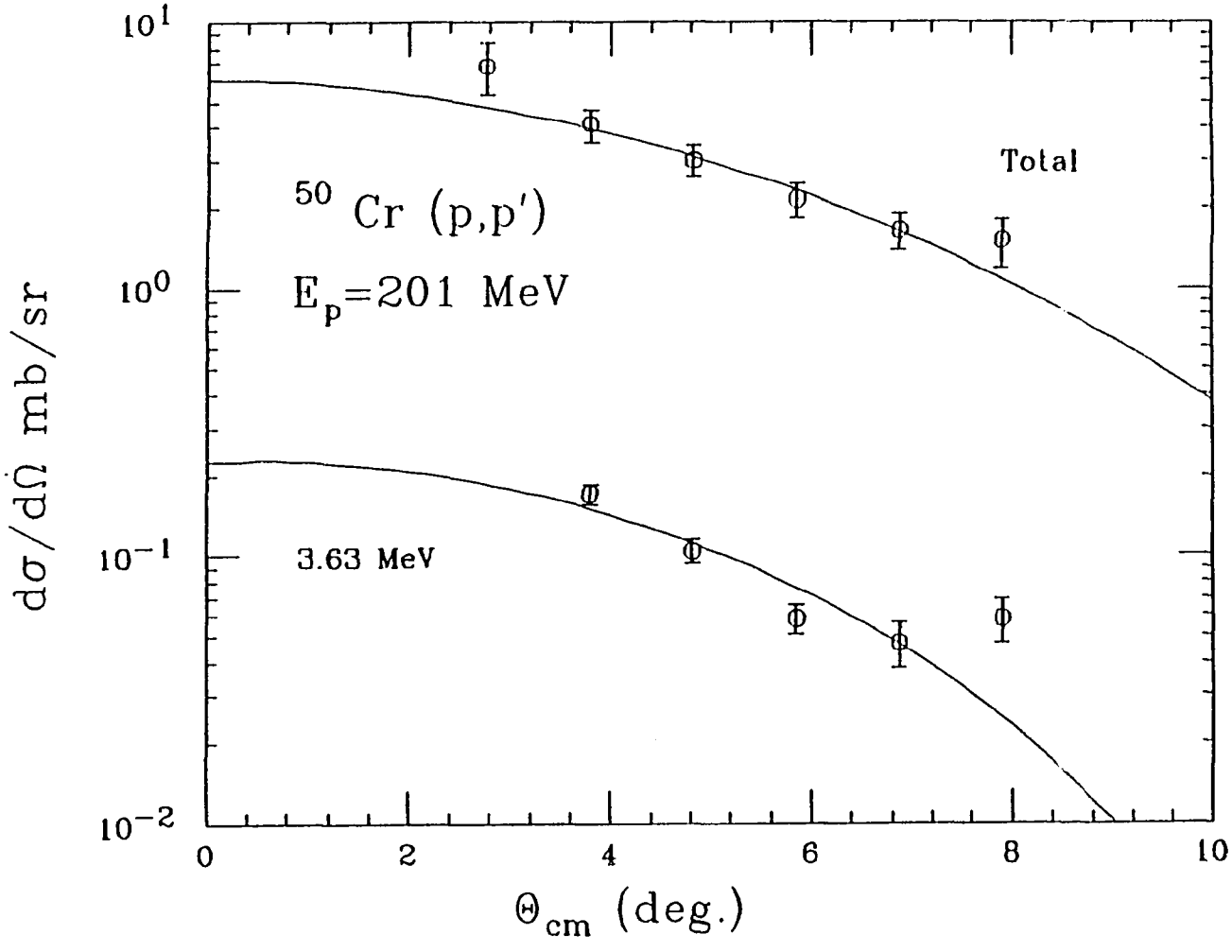
10^1
10^0
10^{-1}
10^{-2}
$d\sigma/d\Omega$ mb/sr
^{50} Cr (p,p')
E_p=201 MeV
Total
3.63 MeV
0
2
4
6
8
10
Θ_{cm} (deg.)